

APPENDIX A1

DETAILED EXPERIMENTAL DATA SETS FOR THE BENCHMARKS

A.1.1. SANA-1

A.1.1.1. Material Data

The pebbles within the test facility are made of non-irradiated graphite Type: Sigri/AL 2-500, with a heat conductivity of:

$$\vartheta \quad \text{in } [^{\circ}\text{C}];$$
$$\lambda \quad \text{in } \left[\frac{\text{W}}{\text{m}\cdot\text{K}}\right];$$
$$\lambda_{\text{AL 2-500}} = 186,021 - 39,5408 \cdot 10^{-2} \cdot \vartheta + 4,8852 \cdot 10^{-4} \cdot \vartheta^2 - 2,91 \cdot 10^{-7} \cdot \vartheta^3 + 6,6 \cdot 10^{-11} \cdot \vartheta^4$$

The heat conductivity data of the fibre insulation modules at the top are represented in air by the formula:

CERACHEM - Blanket; Fa. Gossler:

$$\lambda_{\text{IOB}} = 0,0984 - 2,02 \cdot 10^{-4} \cdot \vartheta + 4,1 \cdot 10^{-7} \cdot \vartheta^2 + 10^{-10} \cdot \vartheta^3;$$

For the bottom insulation the thermal conductivity in air is represented by the following formulas:

Light fire brick RI 30 B; Savoie Feuerfest:

$$\lambda_{\text{IU1}} = 0,396 + 2,46 \cdot 10^{-4} \cdot \vartheta + 2,5 \cdot 10^{-7} + 10^{-10} \cdot \vartheta^3;$$

CERAFORM 1000 and CERABORD 100; Gossler:

$$\lambda_{\text{IU2,3}} = 0,0437 + 7,1 \cdot 10^{-5} \cdot \vartheta + 5 \cdot 10^{-8} \cdot \vartheta^2 + 7 \cdot 10^{-11} \cdot \vartheta^3;$$

THERMOSIL 1100; Gossler:

$$\lambda_{\text{IU4}} = 0,0803 + 4 \cdot 10^{-5} \cdot \vartheta + 7 \cdot 10^{-8} \cdot \vartheta^2;$$

THERMOSIL 1000; Gossler:

$$\lambda_{\text{IU5}} = 0,041 + 4,5 \cdot 10^{-5} \cdot \vartheta + 1,1 \cdot 10^{-7} \cdot \vartheta^2 + 5,5 \cdot 10^{-11} \cdot \vartheta^3;$$

GOSSLEROC GMP 100; Gossler:

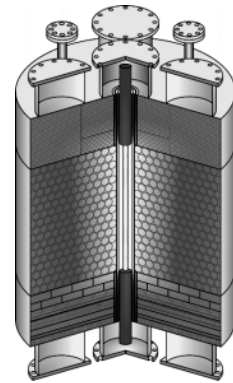
$$\lambda_{\text{IU6}} = 0,058 + 10^{-6} \cdot \vartheta + 4 \cdot 10^{-7} \cdot \vartheta^2;$$

NOTE: Following KFA-experiments the values for the fibre insulation (layer (6) at the bottom and at the top-insulation) are in helium-atmosphere three times higher than those in air!!!

A.1.1.2. Data for The Stationary Tests with Long Heating Element 60mm Pebble Diameter

1. Nitrogen 30kW nominal heating power 60mm pebble diameter
2. Nitrogen 10kW nominal heating power 60mm pebble diameter
3. Helium 30kW nominal heating power 60mm pebble diameter
4. Helium 10kW nominal heating power 60mm pebble diameter

Fig. 1: Arrangement of the heating element <



1. Nitrogen 30kW nominal heating power with long heating element

P heating element/kW	27,189
P electrodes/kW	1,817

Date	20.10.95
Zeile	92
P / kW	30,0
CO / Vol.%	0,58
OXOR 6N / Vol.%	-0,08
TU / °C	26,2
Dewpoint	-43,5

Cooling Water Instrumentation

Thermocouple- Position	Top		Bottom	
	Inlet	Outlet	Inlet	Outlet
Temperature / °C	16,5	25,4	16,2	25,0
Throughput / l/h	220	240	210	210

Arrangement of the Thermocouples

Height / Radius [cm]	6,5	10	22	34	46	58	70	75,6
167	99							
140	60						76	
113	815				523		288	
97	877				663		424	
91	1141	1014	850	750	649	539	452	297
50	1118	953	784	682	582	470	377	269
9	1071	877	709	566	458	366	282	194
3	692				446		240	
-13	665				433		189	
-40	101						24	
-67	49							
Protection Tube	Pebble Bed		Insulation		Vessel Surface			

2. Nitrogen 10kW nominal heating power with long heating element

P heating element/kW	8,855
P electrodes/kW	0,662

Date	13.10.95
Zeile	120
P / kW	10,0
CO / Vol.%	0,04
OXOR 6N / Vol.%	-0,04
TU / °C	26,3
Dewpoint	-31,5

Cooling Water Instrumentation

Thermocouple- Position	Top		Bottom	
	Inlet	Outlet	Inlet	Outlet
Temperature / °C	17,1	22,0	16,9	21,0
Throughput / l/h	200	210	200	220

Arrangement of the Thermocouples

Height / Radius [cm]	6,5	10	22	34	46	58	70	75,6
167	67							
140	39				49			
113	443				268		153	
97	470				347		243	
91	648	563	435	370	315	269	232	156
50	593	465	323	263	220	188	165	125
9	497	344	228	175	147	128	108	84
3	214				141		97	
-13	232				139		78	
-40	59						24	
-67	31							
Protection Tube	Pebble Bed		Insulation		Vessel Surface			

3. Helium 30kW nominal heating power with long heating element

P heating element /kW	27,189
P electrodes /kW	1,817

Date	08.11.95
Zeile	90
P / kW	30,1
CO / Vol.%	0,70
OXOR 6N / Vol.%	0,26
TU / °C	26,0
Dewpoint	-48,4

Cooling Water Instrumentation

Thermocouple- Position	Top		Bottom	
	Inlet	Outlet	Inlet	Outlet
Temperature / °C	14,7	26,8	15,3	25,5
Throughput / l/h	215	170	235	190

Arrangement of the Thermocouples

Height / Radius [cm]	6,5	10	22	34	46	58	70	75,6
167	104							
140	67						74	
113	678				388		206	
97	768				538		310	
91	1052	926	749	644	540	432	352	247
50	1047	894	724	629	531	427	345	268
9	1012	850	700	579	489	401	308	229
3	688				479		262	
-13	624				426		199	
-40	105						21	
-67	45							
Protection Tube	Pebble Bed		Insulation		Vessel Surface			

4. Helium 10kW nominal heating power with long heating element

P heating element /kW	8,855
P electrodes /kW	0,662

Date	27.10.95
Zeile	97
P / kW	10,0
CO / Vol.%	0,02
OXOR 6N / Vol.%	0,25
TU / °C	23,0
Dewpoint	-44

Cooling Water Instrumentation

Thermocouple- Position	Top		Bottom	
	Inlet	Outlet	Inlet	Outlet
Temperature / °C	16,3	21,3	16,2	20,9
Throughput / l/h				

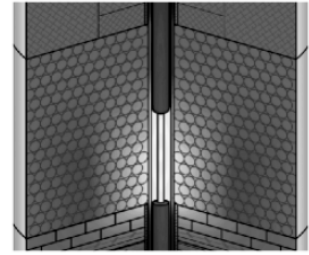
Arrangement of the Thermocouples

Height / Radius [cm]	6,5	10	22	34	46	58	70	75,6
167	66							
140	40						45	
113	341				188		104	
97	387				262		151	
91	565	488	372	311	256	203	168	124
50	552	450	337	284	233	187	157	130
9	491	389	301	240	201	166	132	105
3	290				194		116	
-13	276				180		92	
-40	62						22	
-67	29							
Protection Tube	Pebble Bed		Insulation		Vessel Surface			

A.1.1.3. Data for The Stationary Tests with Short (Half) Heating Element on The Bottom Side

1. Nitrogen 20kW nominal heating power
2. Helium 20kW nominal heating power

Fig. 2: Arrangement of the heating element <



1. Nitrogen 20kW nominal heating power with short (half) heating element on the bottom side

P heating element /kW	16,17
P electrodes /kW	2,783

Date	27.02.96
Zeile	39
P / kW	20,1
CO / Vol.%	0,33
OXOR 6N / Vol.%	-999,99
TU / °C	27,5
Dewpoint	-48,1

Cooling Water Instrumentation

Thermocouple- Position	Top		Bottom	
	Inlet	Outlet	Inlet	Outlet
Temperature / °C	10,5	17,7	11,2	22,0
Throughput / l/h				

Arrangement of the Thermocouples

Height / Radius [cm]	6,5	10	22	34	46	58	70	75,6
167	40							
140	43				59			
113	479			336			195	
97	555			459			315	
91	621	600	554	509	455	384	322	210
50	925	785	613	522	432	342	274	197
9	1073	792	590	433	332	263	203	146
3	567			316			177	
-13	575			328			141	
-40	93				50			
-67	46							
Protection Tube	Pebble Bed		Insulation		Vessel Surface			

2. Helium 20kW nominal heating power with short (half) heating element on the bottom side

P heating element /kW	16,17
P electrodes /kW	2,783

Date	10.02.96
Zeile	87
P / kW	20,0
CO / Vol.%	-0,02
OXOR 6N / Vol.%	999,99
TU / °C	24,3
Dewpoint	-21

Cooling Water Instrumentation

Thermocouple- Position	Top		Bottom	
	Inlet	Outlet	Inlet	Outlet
Temperature / °C	11,4	18,4	12,0	23,0
Throughput / l/h				

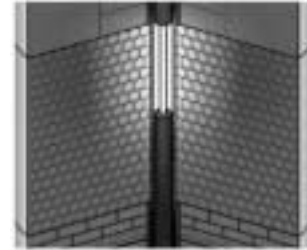
Arrangement of the Thermocouples

Height / Radius [cm]	6,5	10	22	34	46	58	70	75,6
167	35							
140	44				53			
113	344			222			129	
97	418			320			200	
91	493	468	419	379	329	270	222	160
50	794	689	530	460	380	303	246	193
9	986	779	607	478	389	310	235	175
3	595			380			201	
-13	555			352			158	
-40	98				55			
-67	40							
Protection Tube	Pebble Bed		Insulation		Vessel Surface			

A.1.1.4. Data for The Stationary Tests with Short (Half) Heating Element on The Top Side

1. Nitrogen 20kW nominal heating power
2. Helium 20kW nominal heating power

Fig. 3: Arrangement of the heating element <



1. Nitrogen 20kW nominal heating power with short (half) heating element on the top side

P heating element /kW	16,17
P electrodes /kW	2,783

Date	18.12.95
Zeile	7
P / kW	20,0
CO / Vol.%	0,36
OXOR 6N / Vol.%	0,04
TU / °C	28,0
Dewpoint	-49

Cooling Water Instrumentation

Thermocouple- Position	Top		Bottom	
	Inlet	Outlet	Inlet	Outlet
Temperature / °C	13,5	22,7	13,6	19,2
Throughput / l/h				

Arrangement of the Thermocouples

Height / Radius [cm]	6,5	10	22	34	46	58	70	75,6	
167	92								
140	53				63				
113	734			428		229			118
97	775			546		356			217
91	1082	923	726	613	514	420	353	233	
50	793	616	486	400	343	288	247	184	
9	425	341	278	237	207	183	154	117	
3	265			199		137			95
-13	264			189		106			66
-40	73				48				
-67	32								
Protection Tube	Pebble Bed		Insulation		Vessel Surface				

2. Helium 20kW nominal heating power with short (half) heating element on the top side

P heating element /kW	16,17
P electrodes /kW	2,783

Date	19.01.96
Zeile	77
P / kW	20,0
CO / Vol.%	0,55
OXOR 6N / Vol.%	-999,99
TU / °C	24,2
Dewpoint	-47,6

Cooling Water Instrumentation

Thermocouple- Position	Top		Bottom	
	Inlet	Outlet	Inlet	Outlet
Temperature / °C	11,7	21,8	12,4	19,3
Throughput / l/h				

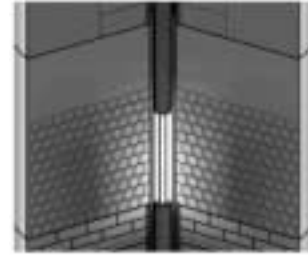
Arrangement of the Thermocouples

Height / Radius [cm]	6,5	10	22	34	46	58	70	75,6	
167	96								
140	56				58				
113	613			323		164			99
97	695			441		247			168
91	1012	860	655	539	435	337	269	190	
50	761	622	503	420	352	282	233	186	
9	431	382	341	297	261	222	177	140	
3	330			252		154			117
-13	298			223		119			78
-40	78				52				
-67	31								
Protection Tube	Pebble Bed		Insulation		Vessel Surface				

A.1.1.5. Data for The Stationary Tests with Short (Half) Heating Element on The Bottom Side and a Gas Plenum above The Pebble Bed

1. Nitrogen 20kW nominal heating power
2. Helium 20kW nominal heating power

Fig. 4: Arrangement of the heating element and the pebble bed <



1. Nitrogen 20kW nominal heating power with short (half) heating element on the bottom side and a gas plenum above the pebble bed

P heating element /kW	16,17
P electrodes /kW	2,783

Dateiname: sn20o109

Date	24.07.95
Zeile	23
P / kW	20,1
CO / Vol.%	0,20
OXOR 6N / Vol.%	-0,05
TU / °C	31,9
Dewpoint	-33,5

Cooling Water Instrumentation

Thermocouple- Position	Top		Bottom	
	Inlet	Outlet	Inlet	Outlet
Temperature / °C	20,6	26,0	20,7	29,2
Throughput / l/h				

Arrangement of the Thermocouples

Height / Radius [cm]	6,5	10	22	34	46	58	70	75,6	
167	69								
140					45				63
113			346		241		165		113
91									194
63	615	543	456	319		254		207	
50	776	665	502	421	347	287	243	183	
9	937	727	510	355	266	214	169	126	
3			487		252		148		103
-13			495		267		120		74
-40					100				57
-67	31								
Protection Tube	Pebble Bed		Insulation		Vessel Surface				

2. Helium 20kW nominal heating power with short (half) heating element on the bottom side and a gas plenum above the pebble bed

P heating element /kW	16,17
P electrodes /kW	2,783

Date	8.8.95
Zeile	23
P / kW	20,0
CO / Vol.%	-0,01
OXOR 6N / Vol.%	2,09
TU / °C	30,2
Dewpoint	-3,1

Cooling Water Instrumentation

Thermocouple- Position	Top		Bottom	
	Inlet	Outlet	Inlet	Outlet
Temperature / °C	22,2	29,8	22,4	35,6
Throughput / l/h				

Arrangement of the Thermocouples

Height / Radius [cm]	6,5	10	22	34	46	58	70	75,6	
167	73								
140					50				62
113			287		201		138		104
91									164
63	546	496	411	283		200		185	
50	697	603	460	394	328	266	220	180	
9	893	732	561	437	351	278	211	161	
3			553		341		180		137
-13			519		321		147		94
-40					107				64
-67	31								
Protection Tube	Pebble Bed		Insulation		Vessel Surface				

A.1.1.6. Data for The Stationary Tests with Long Heating Element, 30mm Pebble Diameter

1. Helium 30kW nominal heating power 30mm pebble diameter
1. Helium 10kW nominal heating power 30mm pebble diameter
2. Nitrogen 30kW nominal heating power 30mm pebble diameter
3. Nitrogen 10kW nominal heating power 30mm pebble diameter

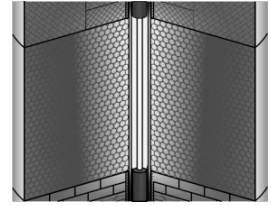


Fig. 5: Arrangement of the heating element and the pebble bed <

1. Nitrogen 30kW nominal heating power with long heating element and 30mm pebble diameter

P heating element /kW	27,189
P electrodes /kW	1,817

Date	03.05.96
Zeile	16
P / kW	30,0
CO / Vol. %	0,34
OXOR 6N / Vol. %	0,01
TU / °C	30,5
Dewpoint	-42,1

Cooling Water Instrumentation

Thermocouple- Position	Top		Bottom	
	Inlet	Outlet	Inlet	Outlet
Temperature / °C	16,8	36,8	17,9	32,4
Throughput / l/h		200		200

Arrangement of the Thermocouples

Height / Radius [cm]	8,5	11	22	34	46	58	70	75,6
167	64							
140	68						67	
113	960				589		299	
97	1026				816		419	
91	1296	1207	1023	889	767	600	416	270
50	1269	1208	1019	840	717	561	390	276
9	1153	1122	979	816	666	502	302	217
3	958				617		313	
-13	875				599		235	
-40	116						63	
-67	70							
1. Pebble to Protection Tube		Pebble Bed		Insulation		Vessel Surface		

2. Nitrogen 10kW nominal heating power with long heating element and 30mm pebble diameter

P heating element /kW	8,855
P electrodes /kW	0,662

Date	28.03.96
Zeile	22
P / kW	10,0
CO / Vol. %	0,18
OXOR 6N / Vol. %	-0,1
TU / °C	27,3
Dewpoint	-29,5

Cooling Water Instrumentation

Thermocouple- Position	Top		Bottom	
	Inlet	Outlet	Inlet	Outlet
Temperature / °C	14,9	20,3	14,6	19,5
Throughput / l/h		200		200

Arrangement of the Thermocouples

Height / Radius [cm]	8,5	11	22	34	46	58	70	75,6
167	41							
140	39						45	
113	538				325		168	
97	592				471		245	
91	756	705	579	498	422	331	227	148
50	710	660	489	353	285	234	166	127
9	516	482	346	226	166	134	95	80
3	310				145		93	
-13	310				161		75	
-40	62						39	
-67	37							
1. Pebble to Protection Tube		Pebble Bed		Insulation		Vessel Surface		

3. Helium 30kW nominal heating power with long heating element and 30mm pebble diameter

P heating element /kW	27,189
P electrodes /kW	1,817

Date	30.04.96
Zeile	18
P / kW	30,0
CO / Vol. %	0,38
OXOR 6N / Vol. %	0,09
TU / °c	30,0
Dewpoint	-38,5

Cooling Water Instrumentation

Thermocouple- Position	Top		Bottom	
	Inlet	Outlet	Inlet	Outlet
Temperature / °C	17,2	36,6	18,2	33,1
Throughput / l/h		200		200

Arrangement of the Thermocouples

Height / Radius [cm]	8,5	11	22	34	46	58	70	75,6	
167	68								
140	78						69		
113	778				425		214		115
97	866				632		300		215
91	1155	1076	867	719	594	442	320	243	
50	1159	1096	890	705	590	454	332	269	
9	1045	1014	869	715	584	452	298	240	
3	846				548		313		194
-13	738				497		218		122
-40	119						71		
-67	63								
1. Pebble to Protection Tube		Pebble Bed		Insulation		Vessel Surface			

4. Helium 10kW nominal heating power with long heating element and 30mm pebble diameter

P heating element /kW	8,855
P electrodes /kW	0,662

Date	20.02.95
Zeile	98
P / kW	10,0
CO / Vol. %	-0,01
OXOR 6N / Vol. %	2,08
TU / °c	26,5
Dewpoint	-15,1

Cooling Water Instrumentation

Thermocouple- Position	Top		Bottom	
	Inlet	Outlet	Inlet	Outlet
Temperature / °C	18,9	28,3	19,6	26,7
Throughput / l/h		200		200

Arrangement of the Thermocouples

Height / Radius [cm]	8,5	11	22	34	46	58	70	75,6	
167	41								
140	45						43		
113	382				199		104		63
97	430				299		141		106
91	606	559	429	344	277	203	149	119	
50	614	573	435	324	265	203	153	131	
9	508	488	402	316	251	193	132	112	
3	384				233		137		94
-13	347				223		104		67
-40	72						46		
-67	39								
1. Pebble to Protection Tube		Pebble Bed		Insulation		Vessel Surface			

A.1.2. OKBM EXPERIMENTAL FACILITIES FOR TESTING OF HTGRS COMPONENTS

A.1.2.1. St-1312 High Temperature Gas Test Facility (Fig. 1)

– Purpose

Testing of full-scale models of steam generator and high temperature heat exchangers under operating parameters. Hydraulic and vibrational characteristics of helium and steam-water circuits of steam generators and heat exchangers and thermal state of the structural elements can be studied.

Besides, the facility is used for the development of control and instrumentation system for different types of reactors.

– Main Engineering Data

Coolant	helium
Coolant temperature, °C	up to 965
Coolant pressure, MPa	5,0
Coolant flowrate, kg/s	up to 6,48
Heaters power, MW	15
Steam generator model heat transfer, MW	10
Coolant temperature at steam generator model inlet, °C	up to 750
Coolant temperature at steam generator model outlet, °C	up to 540
Steam pressure at steam generator model outlet, MPa	17,6
Heat exchanger model thermal heat transfer, MW	0-5

The facility consists of the following main systems:

- gas circuit ;
- steam-water circuit ;
- circuit for equipments cooling ;
- control and instrumentation system;
- TV supervision system.

Coolant circuit includes circulator, recuperator, heater, cooler. heat exchanger and steam generator models.

– Status of the facility

Commissioning phase was completed in 1991. The first stage of steam generator model testing at power level up to 20 % was carried out. At present putting of the facility in prolonged storage has been completed.

A.1.2.2. Main Circulator Test Facility St-1383 (Fig. 2)

– Purpose

Testing of a full-scale prototype of the primary circuit gas circulator. The facility serves for testing of gas circulators, valves and equipment used in HTGRs.

Main Engineering Data

Coolant	helium
Maximum coolant flowrate, kg/s	95
Coolant pressure, MPa	4,9
Coolant temperature, °C	345
Coolers heat transfer, kW	1010,0

The facility consists of a circulating gas circuit of 41,5 m³ volume, in a form a cylindrical tank with a built-in gas circulator, and auxiliary systems (of heat removal, lubrication and so on).

– Status of the facility

A full-scale prototype of the gas circulator is fabricated. Start-up and trial operation of the facility under partial loads was performed. At present putting of the facility in prolonged has been completed.

A.1.2.3. St-1565 High Temperature Helium Test Facility (Fig. 3)

– Purpose

Testing of fitting, thermal insulation, relief valve, helium mixer models; study of helium coolant technology, study of thermal and hydraulic parameters of steam generators and heat exchanges models.

Simulation of residual heat removal from the core in the emergencies. Study of heat and mass transfer under depressurization of the primary circuit.

Study of thermal processes under water ingress into the primary circuit. Validation of appropriate codes on the test results will be performed.

– Main Engineering Data

Coolant	helium
Coolant pressure, MPa	up to 5,0
Coolant temperature, °C	up to 1000,0
Coolant flowrate, kg/s	0,1
Electric heater power, kW	up to 500

– Status of the facility

The test facility was put into operation in 1979. A steam generator model was tested. By the present, tests of the prototype shut-off valves (equivalent diameter of 65 mm) used in the pipelines of HTGR refuelling system, of insulation and relief valve have been finished. During the whole period of the facility operation the purification system and control systems of coolant quality are tested. Preliminary tests and analysis of the possibility for investigations of heat and mass transfer in the emergencies were carried out. At present the facility is out of operation.

A.1.2.4. Control Rod Drive Mechanism Test Facility

– Purpose

Testing of the system: “drive mechanism-control rod-drive mechanism guideline”.

– Main Engineering Data

Prototype drive mechanism	full-scale
Operating travel, m	up to 5
Drive mechanism type	electro-mechanic (facility can be adopted for testing another type of drive mechanism - pneumatic, hydraulic)
Medium	atmospheric air

– Status of the facility

The facility is in operation since 1980. Testing of drive mechanisms of different types carried out. At present the facility is out of operation.

A.1.2.5. Masex Test Facility (Fig. 4)

– Purpose

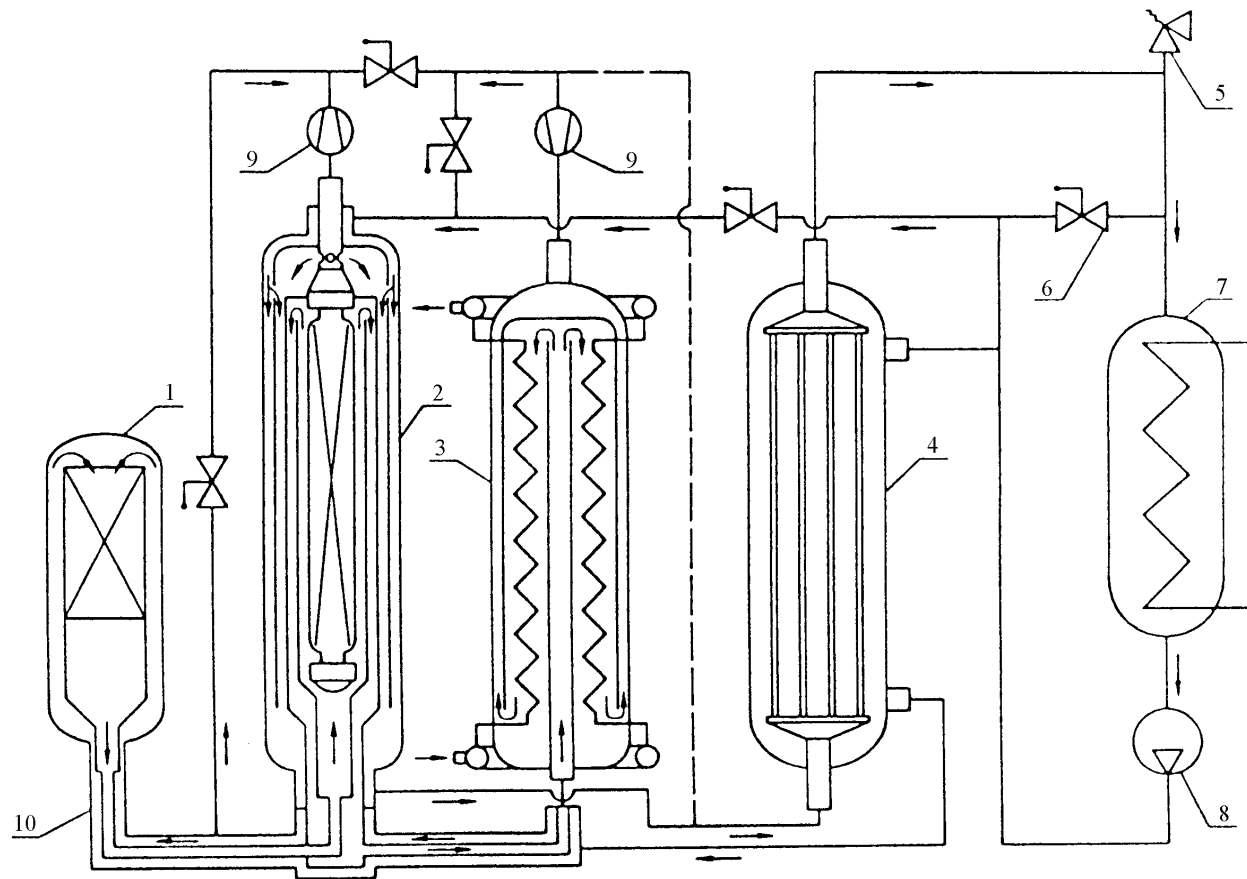
Investigation of heat and mass transfer through penetrations, orifices and tubes. Computational codes validation.

– Main Engineering Data

Tank volume, m ³	0,4
Tubes length, m	up to 1,6
Media taking part in mass exchange	helium-air
Built-in fan's flowrate, m ³ /h	300,0

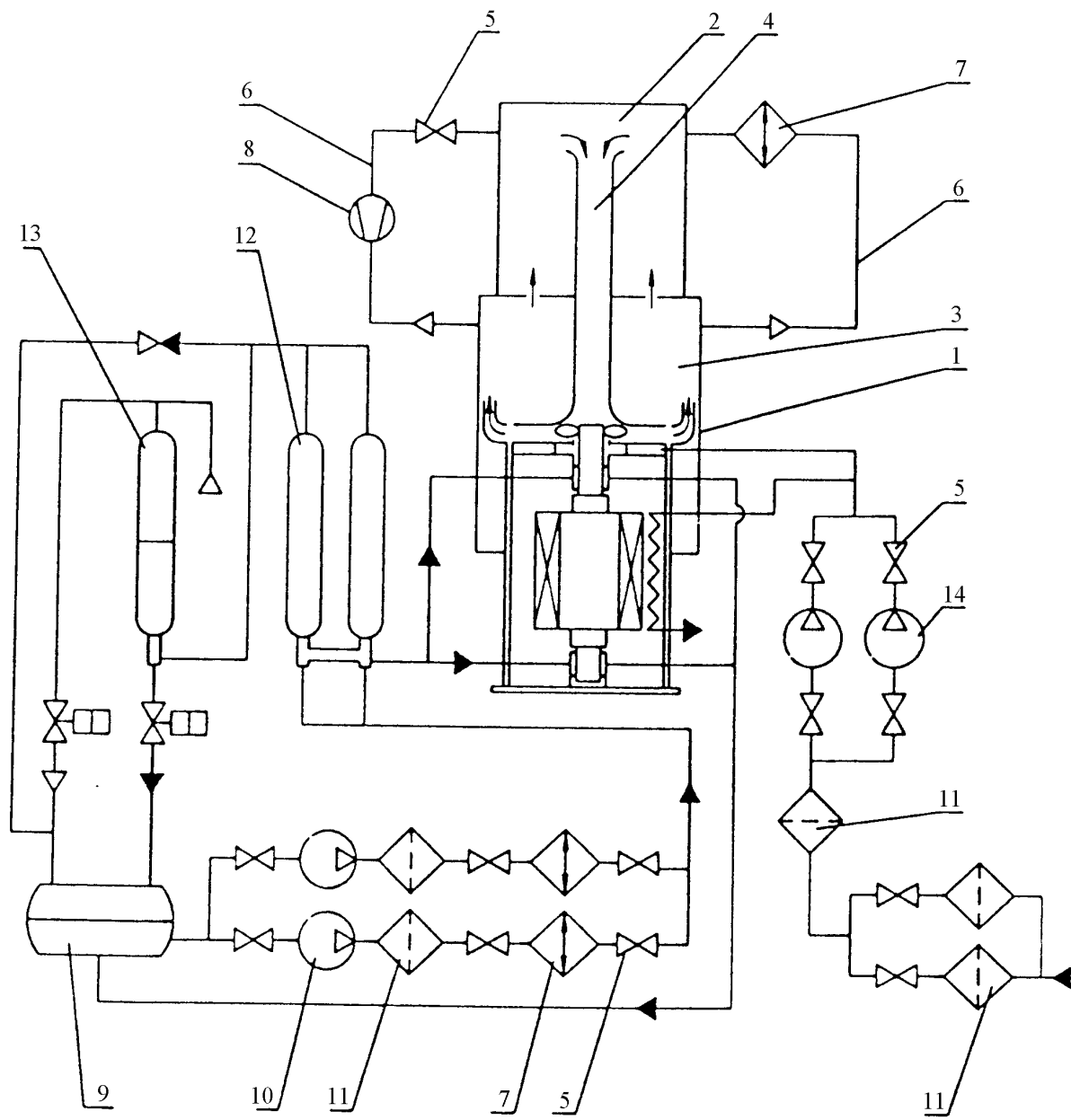
– Status of the facility

Since 1991 mass exchange of helium-air for tubes of different length and slope to the horizon was investigated. Influence of gas circulator operation upon mass exchanger was also investigated. Computational codes were validated. At present the facility is out of operation.



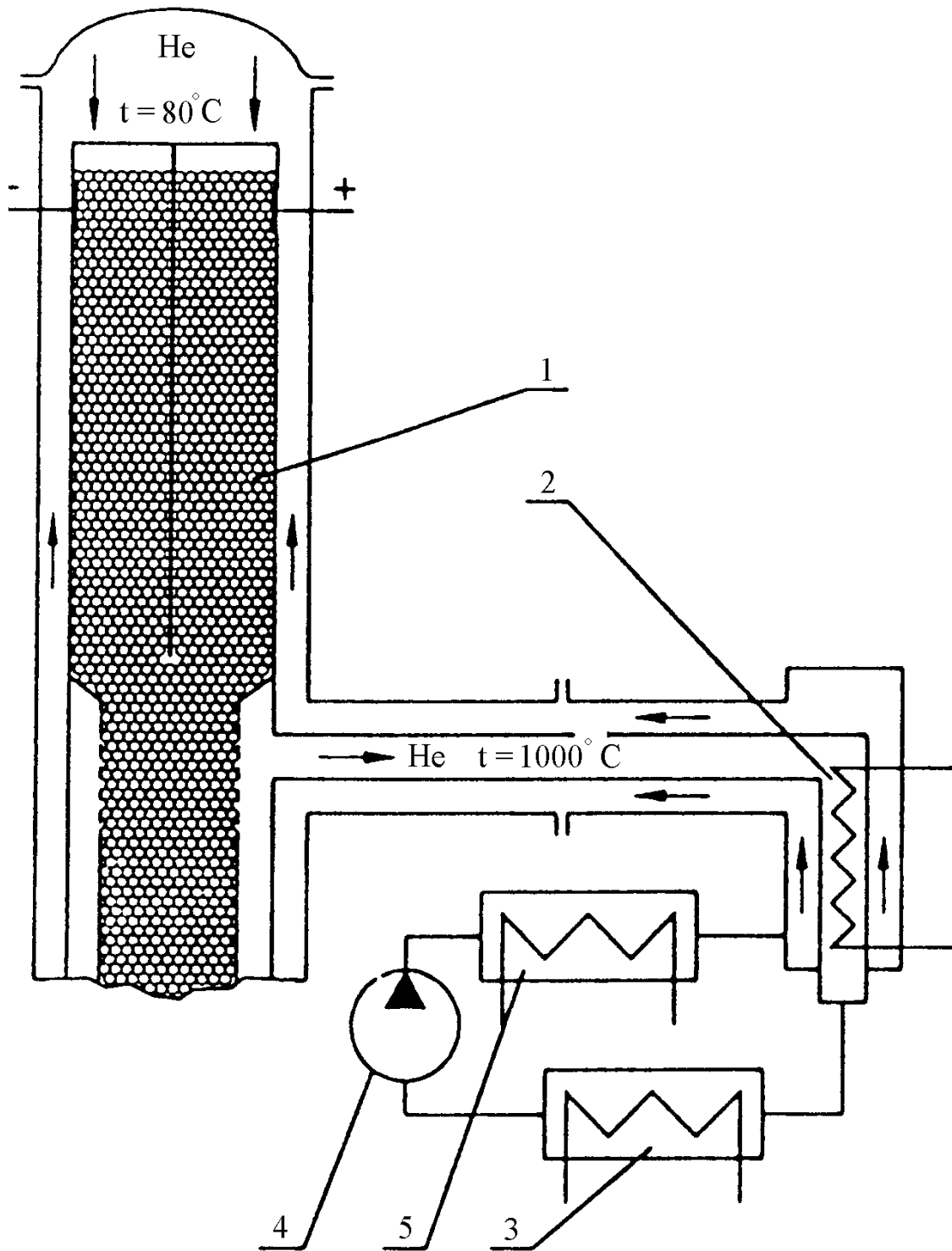
- | | |
|------------------------------------|--------------------|
| 1. High temperature heater | 6. Adjusting valve |
| 2. High temperature heat exchanger | 7. Cooler |
| 3. Steam generator | 8. Gas circulator |
| 4. Recuperator | 9. Flowmeter |
| 5. Relief valve | 10. Double duct |

Fig. 1 (A.1.2.1.) High temperature gas test facility ST-1312 circuit diagram



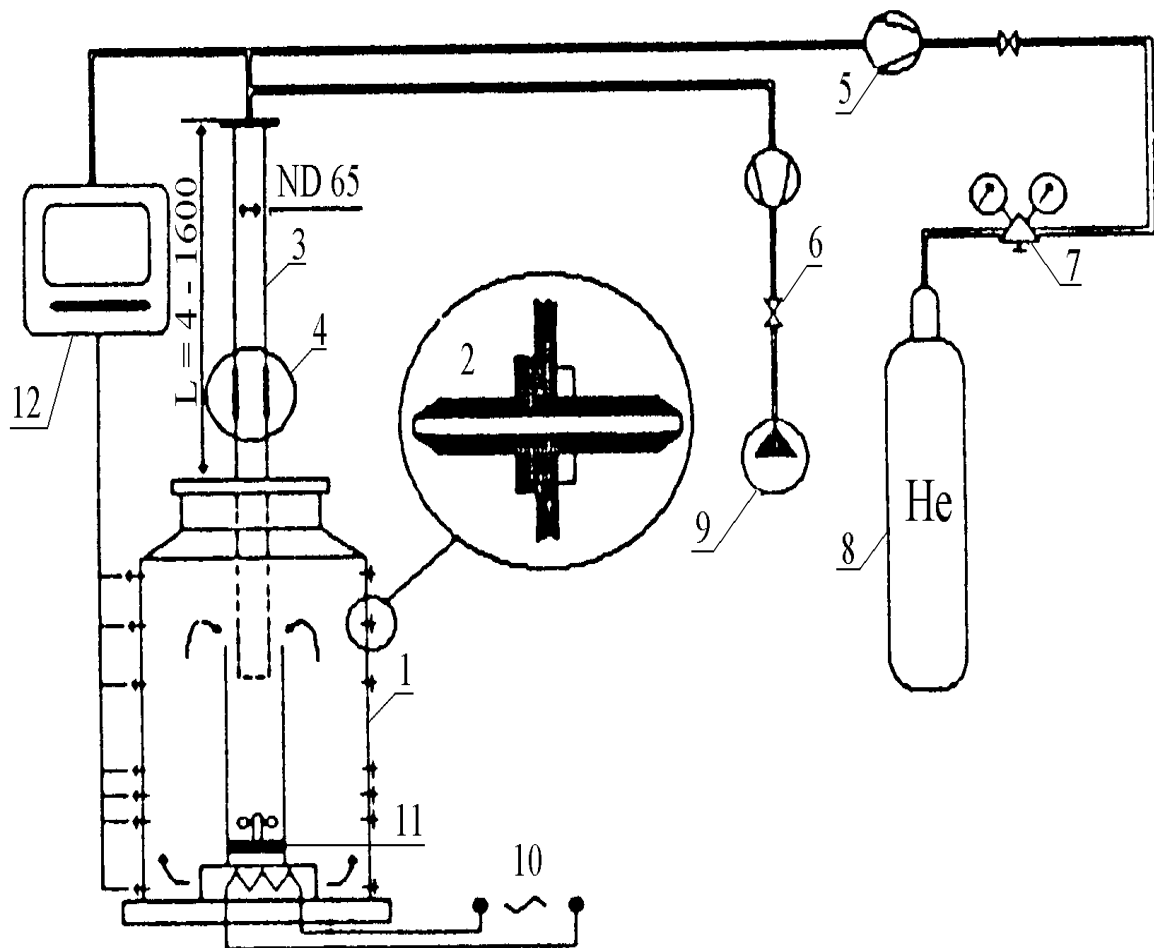
- | | | |
|--------------------|--------------|-------------------------|
| 1. Vessel | 6. Bypass | 11. Filter |
| 2. Suction plenum | 7. Cooler | 12. Oil cylinder |
| 3. Pressure plenum | 8. Flowmeter | 13. Gas-oil accumulator |
| 4. Central duct | 9. Oil tank | 14. Pump |
| 5. Valve | 10. Oil pump | |

Fig. 2 (A.1.2.2.) Diagram of the main circulator test facility ST-1383



1. High temperature electric heater
2. Main cooler
3. Cooler
4. Circulator
5. Heater

Fig. 3 (A.1.2.3.) Outline of high temperature helium test facility ST-1565



- | | | | |
|----------------|--------------------|-----------------------|-----------------------|
| 1. Vessel | 4. Flexible insert | 7. Pressure regulator | 10. Heater |
| 2. Sample pipe | 5. Flowmeter | 8. Cylinder | 11. Gas circulator |
| 3. ND 65 pipe | 6. Valve | 9. Air circulator | 12. Measuring complex |

Fig. 4 (A.1.2.5.) MASEX Experimental facility for mass transfer investigation

APPENDIX A2

CODE DESCRIPTION

A.2.1. DESCRIPTION OF THE CEA TRIO-EF CODE

A.2.1.1. Introduction

TRIO-EF is a general purpose Fluid Mechanics 3D Finite Element Code. The system capabilities cover areas such as steady state or transient, laminar or turbulent, isothermal or temperature dependent fluid flows; it is applicable to the study of coupled thermo-fluid problems involving heat conduction and possibly radiative heat transfer.

The code is widely used for applications in reactor design, safety analysis and final nuclear waste disposal. More recently, it has been used to study the thermal behaviour of the AVLIS process separation module.

A.2.1.2. Physical Models

TRIO-EF is a general purpose finite element code for flow analysis:

- in industrial scale 3 D geometries,
- with or without distributed internal obstacles,
- with incompressible Newtonian fluid with low thermal expansion,
- steady or unsteady,
- under laminar or turbulent (K- ϵ model) conditions,
- through porous media,
- with or without energy coupling
- with phase change: liquid-solid.

Furthermore, TRIO-EF is able to deal with nonlinear heat transfer analysis:

- temperature dependent properties,
- forced, natural and mixed convection,
- radiation exchange in enclosures through non participating media, 2 D and 3 D view factor computation.

A.2.1.3. Salient Features

TRIO-EF is based on a macro-language allowing the user to handle data through named and typed objects such as nodal coordinates, fluid properties, thermal or vector fields. An interpreter translates the user-oriented commands into a coordinated set of operator library management instructions which are transparent to the user. Basically TRIO-EF is a set of independently executable modules and computing tools acting on the objects.

All data items can be defined as parameters, enabling the user to develop his own algorithms through the macro-language. Therefore TRIO-EF is ideally suited to parametric and optimization studies.

TRIO-EF takes advantage of the state of the art software development techniques and Quality Assurance Methodology.

A.2.1.4. Numerical Schemes for Flow Computation

a) Governing equation

The equations solved by TRIO-EF comprise the full set of Navier-Stokes equations using the Business approximation

$$\text{continuity: } \operatorname{div} U = 0 \quad (1)$$

$$\text{Momentum: } DU/Dt = 1/\rho \operatorname{grad} p + \operatorname{div} (\nu \operatorname{grad} U) + g\beta (T-T_0) \quad (2)$$

$$\text{Energy: } DT/Dt = \operatorname{div} (\alpha \operatorname{grad} T) \quad (3)$$

where U , P and T are respectively the velocity, pressure and temperature, and ρ , ν , α , β the density, kinematic viscosity, thermal diffusivity and volumetric thermal expansion coefficient.

g : gravitational acceleration

b) spatial discretization

The equations listed above are discretized by a finite element method for the spatial approximation using the bilinear 4 nodes elements (in 2 D) and trilinear 8 nodes brick (in 3 D) for velocity and temperature. The pressure is constant over an element.

After discretization of the continuity and momentum equations, we obtain the following linear system at time step "n":

$$M U^n - M U^{n-1} + A U^n - C^T P^n = F \quad (4)$$

$$C U^n = 0 \quad (5)$$

where:

- U is the global vector of the nodal velocity components at time n or $n-1$,
- p is the global vector of the element pressure,
- m depends on the algorithm used,
- M is the consistent mass matrix,
- A contains the advection and diffusion operators (the advection operator can be built in various ways).

c) penalty algorithm

If we take $m = n$, the system is solved implicitly. In order to eliminate the pressure, we modify v by writing:

$$P^n = \varepsilon C U^n \quad (6)$$

which leads to:

$$(M/\Delta t + A + \epsilon C^T C) U^n = F + M/\Delta t U^{n-1} \quad (7)$$

where Δt is the time step

Note: for discontinuous pressure elements, the $C^T X$ matrix can be computed at the element level.

The incompressibility constraint is obtained when ϵ is large enough, but not too large (because of round off errors). Typically for 2 D flows, we have: $10^6 < \epsilon L^2/\nu < 10^{10}$. For 3 D flows, we replace L^2 by L^3 in the above formula.

d) The semi-implicit algorithm

If we take $m = n - 1$ and if we diagonalize the mass matrix (using for example a Gauss Lobatto quadrature) the algorithm becomes explicit in the momentum equation. Using the continuity equation, we can eliminate the velocity at the time n and get the following linear system:

$$(CD^{-1}C^T) P^n = -\Delta t CD^{-1} (F - Au^{n-1}) \quad (8)$$

Where D is the lumped mass matrix, which takes into account the Dirichlet boundary conditions on the velocity.

This scheme is conditionally stable.

A.2.1.5. Diffuse Radiative Heat Transfer: Formalism

In many thermal engineering applications, surfaces are separated by radiatively non-participating media and may be idealized as diffuse emitters and reflectors. Consequently, the net radiant energy fluxes are intimately related to purely geometrical quantities called shape factors, that take into account hidden parts: the problem is mainly the shape factor evaluation.

a) Formalism for radiative enclosures

Radiative enclosure are decomposed into elementary surfaces (finite planar polygonal surfaces). The standard radiosity method gives the matrix relationship between the mean radiant fluxes ϕ and the mean temperatures T over the elements, the matrix depending upon the shape factors and the wall total emissivities:

$$\phi = (I - F) (I - (I - \epsilon) F)^{-1} \epsilon \sigma T^4 \quad (10)$$

where:

- I is the identity matrix
- F is the shape factor matrix
- ϵ is the diagonal matrix of the element total emissivities
- σ is the Stefan-Boltzman constant

this relation constitutes a nonlinear boundary condition to the heat conduction equation. The radiant operator is obtained by linearizing equation 10 and by using the relation between nodal temperature and mean temperature.

If $T(i)$ is the nodal temperature at step i , the iterative process which leads to the solution, is as follows:

$$T(i) = K T(i) \quad (11)$$

$$(\phi^{i+1}) = R(\epsilon, F, T(i) K T(i+1)) \quad (12)$$

with:

$$R(\epsilon, F, T(i)) = (I - F) (I - (I - \epsilon) F)^{-1} \epsilon \sigma T(i)^3 \quad (13)$$

then, the radiant operator is introduced into the conductivity operator.

b) Hidden-surface algorithm of shape factors

The method employed for the computation of 3-D shape factors is derived from an algorithm established for synthetic image generation.

The shape factor between two surfaces i and j is defined as the fraction of the radiant energy leaving surface i which strikes surface j . According to the radiative properties of the surface, assumed to be isothermal, the shape factor is reduced to:

$$F_{ij} = \frac{1}{S_{ij}} \int_{S_i} \frac{\cos \Theta_i \cos \Theta_j}{\pi(r_{ij})^2} v_{ij} dS_i dS_j \quad (14)$$

where n_i, n_j, S_i, S_j denote the surface local normals and areas, θ_i and θ_j the angles between the local normals and local direction $M_i M_j$. The v_{ij} term takes into account the possible occlusion of surface j due to intervening surfaces in direction $M_i M_j$ defined by two current points M_i on surface i and M_j on surface j : $v_{ij} = 0$ if there is an occlusion in the local direction $M_i M_j$, $v_{ij} = 1$ if not.

The difficulty stems from the fact that the evaluation of shape factors requires for any pair of surface to sort all other surfaces in order to predict whether they see each other entirely, partially or not at all. The number of operations to perform would thus grow as the cube of the number of elements, which is prejudicial to the method efficiency when this number is high. This is the main reason for working out a more efficient sorting algorithm.

The visibility problem can be tackled as follows: consider a surface i and a current point M_i on this surface. This surface has, from point M_i , a view of its environment across the hemisphere of directions surrounding its normal. The problem is to determine for each direction which surface is visible from point M_i and calculate the corresponding elementary shape factors.

The numerical implementation for this method requires:

- the subdivision of surfaces, defining within each surface a set of view points and corresponding sub-elements,
- the approximation of the hemisphere of directions.

The algorithm is greatly simplified by considering a cubic surface, the center of which is the current view point. Each face of the cube is divided into square regular cells, each cell defining a viewing direction and an elementary solid angle. The number of cells per face is called resolution.

For all surfaces and for each view point on that surface, the algorithm consists in projecting all other surfaces on the projection cube (figure 1). The depth "3" of each corresponding cell, that is the distance between the projected cell and the view point along the cell direction is calculated. The

projection of the entire environment solves simultaneously the problems of visibility in each cell thanks to the depth and numerical calculation of shape factors.

The method warrants the energy conservation principle, with accuracy checked by the resolution and the subdivision of the elements.

A.2.2. DESCRIPTION OF THE VGM-, DUPT-, SM1- AND GTAS-CODES

N.Kuzavkov

**OKB Mechanical Engineering
Nizhny Novgorod
Russia**

A.2.2.3. VGM-CODE

VGM-code is intended for calculations of normal and emergency transients in nuclear power plants with two circuits and reactors cooled by helium.

Simulating regimes include:

- normal operation,
- urgent drop in power due to failure of equipment,
- emergency regimes (inadvertent withdrawal of control rods, inadvertent action of absorber ball
- reactivity system, loss of station service power, violation of heat removal).

Simulating circuits and systems include main equipment having an effect on transients. The mathematical simulation comprises neutronic process, thermal-hydraulic process in the primary, secondary circuits and emergency decay heat removal system, heat transfer in fuel elements, a model of reactivity control system.

The simulation of neutronic process is based on the point kinetics method in 6-group approximation.

Thermal-hydraulic process is simulated in the frame of 1-D model with account of natural convection of the coolant and possibility to change a direction of the circulation. Mixing of flowrates with different temperatures is assumed to be ideal.

The core thermal model allows to compute coolant and moderator temperatures in axial and radial directions versus core inlet temperature, flowrate distribution and power.

Coefficients of heat transfer between gas, fuel and moderator are calculated. Temperature distribution across the moderator due to heat conduction is taken into consideration.

Mass of kernels in every calculating mesh is reduced to point mass of the mesh. Fuel temperature is computed with account of fuel heat capacity and heat exchange with coolant and moderator.

Total reactivity covers temperature effects of fuel and moderator, reactivity of control system and other reactivity perturbation given by piecewise-linear functions. Core power density distribution, reactivity coefficients, characteristics of control rods are derived from neutronic calculations as input data.

Fuel, moderator and coolant temperatures are averaged on corresponding formulae.

Mathematical model of reactor control and protection system simulates operation of automatic regulator on relay principle. Mathematical model of protection system takes account of possible time delay at formation of shutdown signals, acceleration time of absorber rods and balls.

Differential equations in partial derivatives to provide computation of heat transfer in the core are approximated by stable monotonous difference schemes. After manipulations the closed set of algebraic equations are solved by a run method.

To obtain a level of neutron flux, the set of differential equations of neutron kinetics is solved by the finite difference method. Change of decay heat versus time is given in the form of a Table.

To compute heat transfer and friction coefficients approved formulae are applied. The range of definition of coolant properties is from 280K to 1800K and from 0.01 MPa to 100 MPa.

Input data for the code is a nuclear power plant configuration, thermal properties of materials, core power density distribution, local coefficients of reactivity, distribution of hydraulic resistance, characteristics of control and other systems.

Emergency transients are simulated by violation of reactivity and (or) position of control rods, the given power in the control system of neutron power, temperature and flowrate of the coolant at the inlet of the secondary circuit equipment, temperature and flowrate of the coolant at the inlet of emergency heat exchangers in the secondary circuit.

VGM-code allows to get core power density, temperature distribution in fuel elements, coolant temperatures and flowrates in primary, secondary and emergency cooling circuits.

The code consists of units what are convenient for further improvement. The data bank contains separate blocks and every software module has own input data.

A.2.2.2. DUPT-code

Analysis of temperature and velocity distributions in gas cavities is carried out on two-dimensional DUPT-code. The code includes heat and mass transfer equations on the basis of Business approximation for two-dimensional and axis symmetrical geometries using numerical method of longitudinal and transverse run with variable coefficients. To provide calculations for regions tight-packed with equipment, the code applies porosity body method. In accordance with this method thermal properties of a mesh medium are calculated proportionally with volume parts of the mesh components, cross section for fluid is proportional to the mesh fluid part.

To solve hydrodynamic problem, axial and radial components of fluid velocities on hard boundary are assumed to be equal zero. At initial moment of time the fluid is stationary and velocities in all points of the region are equal to zero. To solve heat problem, temperature of the surroundings and heat transfer coefficients on the boundaries are given.

The heat transferred from one surface to another is determined on the following equation:

$$Q_{12} = eC_o \left[\left(\frac{T_1}{100} \right)^4 - \left(\frac{T_2}{100} \right)^4 \right] \int_{F_1} dF_1 \int_{F_2} \frac{\cos \varphi_1 \cos \varphi_2}{\pi^2} dF_2$$

- e - emissivity;
- C_o - emissivity of black surface;
- T₁, T₂ - temperatures of the surfaces;
- w - angle at a point of surface 1 for dF of the surface 2;
- j₁, j₂ - angles between normals and lines connecting two points on the surfaces 1 and 2;
- r - distance between the two points on the surfaces 1 and 2.

A.2.2.3. SM1-code

The code is based on solution of the energy equation for elements with boundary conditions of the third type. Fluid flow is not computed, account for heat transport by the fluid is provided by means of boundary conditions.

The region to be calculated is divided into elements for which the energy balance equation is solved:

$$m_i c_i \frac{dT_i}{d\tau} = \sum_j k_{i,j} F_{i,j} \Delta T_{i,j} + \sum_n \alpha_{\text{eff } i,n} F_{i,n} \Delta T_{i,n} + N_i$$

where

- m - mass of an element, kg
- c - specific heat, J/kgK
- T - temperature, °C
- t - time, s
- k - heat transfer coefficient, W/m²K
- F - area, m²
- dT - temperature difference, K
- a_{eff} - coefficient of effective heat transfer conductance, W/m²K
- N - power, W
- i - index of an element
- j - index of an element adjacent to i-th element
- n - index of a boundary adjacent to i-th element.

Coefficient of effective heat transfer conductance includes radiative and convective partials

$$a_{\text{eff}} = a_r + a_c$$

During computation of heat transfer by radiation interacting surfaces is assumed to be at right angles to each other, therefore angle distribution of radiative heat is ignored.

a_r is given by

$$a_r = \frac{C_{\text{oe}}}{\Delta T_{1,2}} (T_1^4 - T_2^4),$$

where

- C_o - Stefan - Boltzmann constant, W/m²K⁴
- e - effective emissivity
- T - temperature, °C

$$e = \frac{1}{\frac{1}{\epsilon_1} + \left(\frac{1}{\epsilon_2} - 1 \right) \frac{F_1}{F_2}}$$

- e_{1,2} - emissivity of the surface
- F_{1,2} - area of the surface, m²
- 1,2 - surface number.

Heat transfer by convection is described by

$$\alpha_c = \frac{1}{\left(\frac{1}{\alpha_{m,1} F_1} + \frac{1}{\alpha_{m,2} F_2} \right) F_{1(2)}}$$

where

- a - heat transfer conductance coefficient, W/m²K
- m - index of media adjacent to surfaces 1,2.

For calculation of heat transfer coefficient under natural convection at vertical and horizontal surfaces the equation is used

$$Nu_f = a(Gr_f Pr_f)^b (Pr_f/Pr_s)^{0,25},$$

where

- Nu - Nusselt number
- Gr - Grashof number
- Pr - Prandtl number
- a,b - coefficients depending on surface orientation and magnitude of Gr_fPr_f
- f - index of fluid (Nu, Gr, Pr at parameters of the fluid)
- s - index of surface (Pr at temperature of the surface).

A.2.2.4. GTAS code

The core thermohydraulic calculation was performed using “GTAS” code.

The code is intended for calculation of a temperature state of core and reactor structures in stationary and dynamic modes in two-dimension (R-Z geometry) approximation.

The following data are used as initial data:

- geometric characteristics in the field under consideration;
- distribution of energy releases in structural materials;
- thermophysical properties of structural materials and gas media;
- change of mode parameters.

When developing the program the equation of energy for a porous body was used which without account of the coolant motion energy is of a form:

$$c\rho \frac{\partial T}{\partial \tau} = \text{div}(\lambda_{ef} \text{grad} T) + q_v - c_2 \rho_2 (\vec{w} \cdot \text{grad} T_2)$$

where:

- c - specific heat capacity of porous body;
- ρ - density of porous body;
- T - temperature of porous body;
- τ - time;
- λ_{ef} - effective coefficient of heat conductivity of porous body;
- q_v - density of volumetric energy release;
- c_g - specific heat capacity of gas at constant pressure;
- ρ_g - density of gas;
- T_g - temperature of gas;

\rightarrow
($\mathbf{w} \cdot \text{grad} T_2$) - scalar product of velocity gradient of gas temperature.

Volumetric heat conductivity of porous body is determined from the ratio:

$$c\rho = c_g \cdot \rho_g \cdot \varepsilon + c_o \cdot \rho_o (1 - \varepsilon),$$

where:

ε - relative fraction of gas;
 c_o - specific heat capacity of solid component;
 ρ_o - density of solid component of porous body.

In the structure of graphite blocks considered as a porous body, $c_o \cdot \rho_o \gg c_2 \cdot \rho_g$. Volumetric heat capacity of a porous body depends insignificantly on the kind of gas, density of gas is determined by a density and heat capacity of solid component.

The effective coefficient of heat conductivity of a porous body corresponds to coefficient of heat conductivity for joint heat transfer of energy by radiation between surfaces and by heat conductivity for solid phase and gas.

The equation of energy is solved by a method of balance in two-dimensional approximation. Volume of a region under consideration is divided into calculation elements which have a form of cylinder or a hollow cylinder.

Each calculation element is described by three numerals. The first numeral denotes the type of a calculation element, other numerals denote the number of material in the Table where thermophysical properties are given.

The following types of calculation elements are envisaged:

- 1 - structure of fuel element;
- 2 - structure of graphite blocks;
- 3 - solid body;
- 4 - stagnant transparent gas;
- 5 - stagnant liquid;
- 6 - moving transparent gas;
- 7 - moving liquid.

In the Table of thermophysical properties of materials values of the following parameters are specified for each of the solid porous media depending on the level of temperature:

- coefficient of heat conductivity;
- specific heat capacity;
- density.

For liquid and gases the following is specified:

- coefficient of heat conductivity;
- specific heat capacity at constant pressure;
- density at normal pressure;
- coefficient of dynamic viscosity;
- coefficient of volumetric thermal expansion.

Determination of values of thermophysical parameters is performed using linear interpolation of tabulated values.

Variation of temperature in an annular element under consideration given in Fig. 1 is found from a ratio:

$$\Delta T = (Q1 - Q2 + Q3 - Q4 + Q0 - Q5) \cdot \Delta\tau / (c\rho\Delta V)$$

where:

- ΔT - variation of temperature of element;
- $Q1$ - power delivered through upper boundary of element;
- $Q2$ - power removed through lower boundary of element;
- $Q3$ - power delivered through inner (small) boundary of element;
- $Q4$ - power removed through outer (large) boundary of element;
- $Q0$ - power released in the bulk of element;
- $Q5$ - power removed from the coolant element;
- $\Delta\tau$ - count interval for time;
- $c\rho$ - specific heat capacity and density of material;
- ΔV - volume of element.

Power removed through boundary is determined from the ratio:

$$Q_H = q_{s,k} \cdot F_k$$

where:

- $q_{s,k}$ - density of heat flux through boundary;
- F_k - area of a boundary.

A procedure for calculation of density of heat flux through a boundary is chosen depending on the type of a cell under consideration.

In the case when the cell under consideration and the cell adjoining it consist of porous and solid body the density of heat flux is determined by a ratio:

$$q_{s3} = \frac{2 \cdot (T_{i-1,j} - T_{i,j})}{\left(\frac{\Delta R_{i-1}}{\lambda_{i-1,j}} + \frac{\Delta R_i}{\lambda_{i,j}} \right)}$$

where:

- i - number of element along radius;
- j - number of element along height;
- $i-1$ - number of adjoining element;
- T - temperature;
- ΔR - step of element along radius;
- λ - coefficient of heat conductivity of a material.

For calculation elements consisting of stagnant gas or liquid the density of heat flux is chosen from the ratios:

$$q_{S_3} = \frac{2 \cdot (T_{i-1,j} - T_1)}{(\Delta R_{i-1} / \lambda_{i-1,j})},$$

$$q_{S_4} = \frac{2 \cdot (T_2 - T_{i+1,j})}{(\Delta R_{i+1} / \lambda_{i+1,j})},$$

$$q_{S_{34}} = \varepsilon_g \cdot \lambda_g \cdot \frac{T_1 - T_2}{\Delta R_i} + \sigma_0 \cdot \varepsilon_n \cdot (T_1^4 - T_2^4),$$

$$q_{S_3} \cdot \left(1 - \frac{\Delta R_i}{2 \cdot R_i}\right) = q_{S_{34}} = q_{S_4} \cdot \left(1 + \frac{\Delta R_i}{2 \cdot R_i}\right),$$

where:

T_1, T_2 - temperature of left and right boundaries of an element under consideration;

q_{S_3} - density of heat flux between boundaries of element;

ε_g - coefficient taking into account the impact of convection onto gas layer heat conductivity;

λ_g - coefficient of heat conductivity of gas;

σ_0 - Stefan-Boltzmann constant;

ε_n - emissivity;

R_i - radius on which the element under consideration is set.

Coefficient taking into account the impact of convection in gas layer is determined from a ratio:

$$\varepsilon_c = 0,18 \cdot (Gr \cdot Pr)^{0,25},$$

where:

Gr - Grashof number;

Pr - Prandtl number.

For calculation elements consisting of block structure the coefficient of effective heat conductivity in radial direction was determined by the ratio that is used for small temperature fluctuations in structure which thickness is one block:

$$\lambda_{ef} = \frac{\delta_c + \delta_{bl}}{\left(\frac{\lambda_{bl}}{\delta_c} \varepsilon_c + \sigma_0 \cdot \varepsilon_n \cdot 4 \cdot T^3\right)^{-1} + \delta_{bl} / \lambda_{bl}}$$

where:

δ_c - clearance between blocks;

δ_{bl} - flat-to-flat block dimensions;

T - temperature;

λ_{bl} - block heat conductivity coefficient in radial direction.

In the code heat transfer in axial direction by conductivity is taken into account.

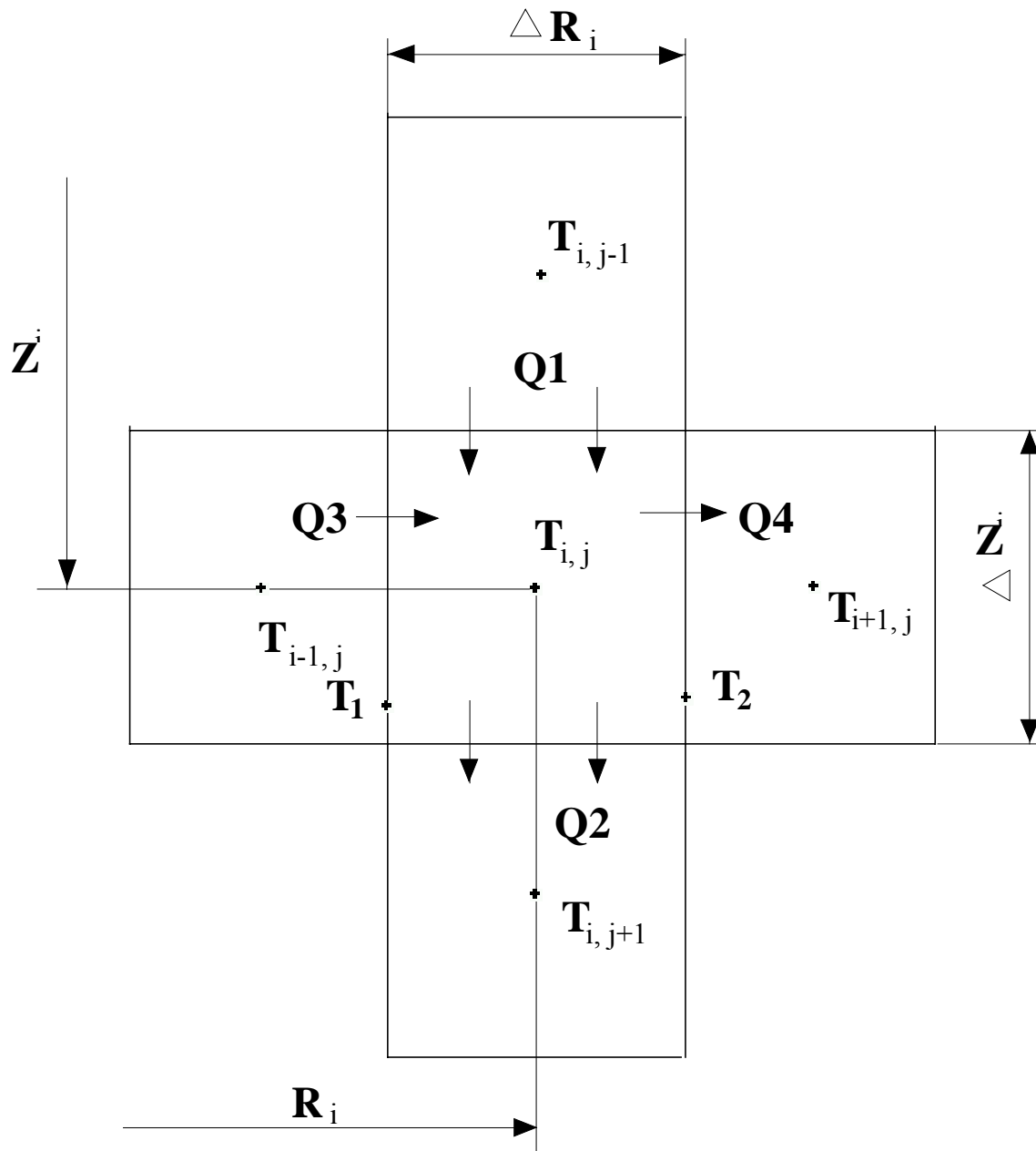


Fig. 1 (A.2.2.) Diagram of calculation element

When the medium under consideration is moving gas the densities of heat flux are determined using the ratios:

$$q_{s3} = \frac{2 \cdot (T_{i-1,j} - T_1)}{(\Delta R_{i-1} / \lambda_{i-1,j})} = \alpha \cdot (T_1 - T_g) + \sigma_0 \cdot \epsilon_n (T_1^4 - T_2^4),$$

$$q_{s4} = \frac{2 \cdot (T_2 - T_{i+1,j})}{(\Delta R_{i+1} / \lambda_{i+1,j})} = \alpha \cdot (T_g - T_2) + \sigma_0 \cdot \epsilon_n^0 (T_1^4 - T_2^4) \left(1 - \frac{\Delta R_i}{R_i}\right),$$

where:

α - coefficient of heat removal from the surface of solid medium to gas;

T_g - temperature of gas.

Power released in the bulk of the element is determined using the ratio:

$$Q_0 = q_v \cdot \Delta V = N_{rel}(\tau) \cdot N_{nom} \cdot K_v(\tau) \cdot \frac{\Delta V}{V},$$

where:

$N_{rel}(\tau)$ - relative variation of power versus time;

N_{nom} - nominal power of reactor;

$K_v(\tau)$ - relative specific heat release in calculation element;

ΔV - volume of an element under consideration.

For calculation of power removed by coolant from the element under consideration the following ratio for heat exchange at constant temperature of porous body solid component is used:

$$Q_5 = (T_s - T_{gin}) \cdot \left(1 - e^{-\frac{kS}{c_g \cdot G_i}}\right) \cdot c_g \cdot G_i,$$

where:

T_s - mean temperature of porous body solid component;

T_{gin} - temperature of gas at the inlet into element;

S - heat exchange surfuel element in the element;

k - coefficient of heat transfer from solid component of porous medium to gas;

c_g - specific heat capacity of gas at constant pressure;

G_i - mass flow of gas through the element.

Two schemes for calculation of heat exchange between porous body solid component and the coolant are intended to be used in the program:

1. When the internal channels are not indicated the heat removal is effected only from the external side of the block by helium flowing through the gaps. Heat transfer coefficient from the graphite of hexagonal block to helium is specified to be equal to heat transfer coefficient of equivalent in area cylinder rod cross section with even energy release distribution from radius with mean temperature along the section.;
2. When coolant channels are specified the heat removal is effected by both helium in gaps with heat transfer coefficient for the first scheme, and helium in channels. The coefficient of heat transfer through the graphite of block to helium in channels is assumed analogous to coefficient of heat transfer through a hollow cylinder without energy releases with inner cooling. Its cross section area is 0.5 of the cell graphite cross section area.

The distribution of flowrate in the slots of graphite structure and cooling channels is found from the solution of a set of equations:

$$\frac{G_i^2}{2F_i^2} \left(\sum_j \frac{\lambda_{ij} \cdot \Delta Z_j}{\rho_{ij} \cdot d_{ij}} + \frac{\xi_i}{\rho_i} \right) + g \sum_j \rho_{ij} \cdot \Delta Z_j = \text{idem},$$

$$\sum_i G_i = G_0,$$

where:

G_i - coolant flow rate in respective channels;

F_i - area of horizontal boundary of calculation element;

λ_{ij} - coefficient of friction resistance in respective channel, related to F_i ;

ρ_{ij} - density of gas;

ΔZ_j - height of calculation element;

d_{ij} - hydraulic diameter;

ξ_i - coefficient of local hydraulic resistance at inlet and outlet from a channel;

G_0 - total flow rate through reactor.

Mass exchange between helium circulating in cooling channels and in gaps is not taken into account.

A.2.3. THE ORNL GRSAC CODE FOR GAS-COOLED REACTOR SIMULATIONS

A.2.3.1. Abstract

An interactive workstation-based simulation code for studying postulated severe accidents in gas-cooled reactors has been developed to accommodate user-generated plant design input with "smart front-end" checking. New code features include on- and off-line plotting, on-line help and documentation, and an automated sensitivity study option. The code and its predecessors have been validated using comparisons with a variety of experimental data and similar codes.

A.2.3.2. Introduction

The GRSAC (Graphite Reactor Severe Accident Code) software is a new general-purpose program developed at Oak Ridge National Laboratory (ORNL). It is based on the ORNL MORECA [1],[2] code for simulating accident scenarios for selected gas-cooled reactor (GCR) design types. The MORECA code and its predecessors were originally developed at ORNL under the sponsorship of the U.S. Nuclear Regulatory Commission (NRC) to perform confirmatory licensing-related studies of a variety of High-Temperature Gas-Cooled Reactor (HTGR) designs, including the Fort St. Vrain HTGR and subsequently the 350-MW(t) steam-cycle Modular HTGR (MHTGR). MORECA was later developed - under U.S. Department of Energy (DOE) sponsorship - to simulate the MHTGR design for the 600 MW(t) direct cycle gas turbine modular helium reactor (GT-MHR).

Since MORECA is a "hard-wired" code, configured only for a particular reactor design, the conversion of MORECA to GRSAC was motivated by the need to generate the connectivities necessary to assemble, verify, and run simulations for a wide variety of graphite-moderated GCR designs.

GRSAC features of particular interest are: three-dimensional core representation, fast-running (typically >2000 times faster than real time on a SUN SparcStation-20 workstation), interactive user interface with on-line and off-line plotting options, automated sensitivity study capabilities, on-line documentation and help screens, and optional ATWS (anticipated transients without scram) capabilities. The basic designs that can be simulated using GRSAC, which the user may modify via the interface to a large (but limited) extent, include the British and French Magnox types (including the Calder Hall, G-2/3, and Bugey-2), Windscale (U.K.), and the HTTR (Japan). Adaptations and analyses are planned for the HTR-10 (China) and the GT-MHR Plutonium burner (U.S.-Russia).

A.2.3.3. Grsac Code Features

A. Reactor Design Setup

Specific design features for a chosen reactor type can be input by the user via design screen selections in the following categories: fuel element, nuclear parameters, core layout and reflector design, primary coolant system, vessel design, reactor cavity, and oxidation parameters. A program setup screen allows the user to activate or deactivate oxidation, Wigner energy, or ATWS features, and to select the coolant gas, core flow direction and computation time parameters. In some cases, such for as the radial and axial power peaking factor inputs and flow coastdown curves, graphical displays and automated consistency check features are included. For all of the user input screens in GRSAC, pop-up HELP windows and a choice of metric or English unit entries are available. The user can also select a "run with validation" option, which is a smart front end check of the entire set of inputs for data inconsistencies.

B. Initial Condition Runs

GRSAC accident sequence analyses require a large set of initial condition values which are created automatically via the Initial Condition mode. The user can select operational inputs such as power level, flow, pressure, etc., and observe the resulting detailed temperature and flow distributions attain steady state conditions. At any point in the run, one can store initial condition values in a RUN file.

C. Programmed Inputs

The interactive input screen for accident simulations allows for user inputs (scram, depressurization, changes in emergency and/or cavity cooling, etc.) at any time during a run. Such inputs can be pre-programmed, however, via a programmed input screen that is available to the user during the run setup procedure.

D. Accident Sequence Runs

Long-term Loss of Forced Convection (LOFC) accidents begin with a programmed flow coastdown transient. They may be simulated both with and without total or partial depressurization of the primary coolant and with or without scram. Optionally, both the active or passive shutdown cooling systems can be made to be either unavailable or available only intermittently in degraded states. For helium or CO₂-cooled cores, there is an option to allow air ingress following a depressurization, and subsequently to initiate (or not) oxidation models for graphite (and clad and metal fuel, if applicable).

LOFC transients in GCRs are generally characterized by slow heatups because of the low power densities and large heat capacities associated with the core.

E. Sensitivity Study Option

Many variations of transient and LOFC accident scenarios have been studied to observe the sensitivities of the predictions to parametric and operational assumptions. These provide guidance in design studies for determining plant operating parameters (including design power level) and in identifying which physical properties and correlations are most crucial to the outcome of postulated accidents.

In the GRSAC automated sensitivity study feature, the rationale is to seek out a set of parameters within user-specified uncertainty bands that result in the worst (or best) case accident consequences using a gradient search algorithm. Sets of 13 model or design parameters (such as heat transfer correlations, etc.) and 12 operational/run parameters (such as time of scram) have been set up to be available for automatic variation (from run to run). The program allows the user to select up to 10 from this set for any given study. To study the effects of a single parameter variation in more detail, a single-parameter option can be used. That parameter is varied uniformly within the uncertainty band (reference run plus 4 others).

A report generator, the results of which are available after the runs are completed, gives a summary of the run results.

A.2.3.4. Description of Selected GrSAC Models

A. Reactor Core and Primary Cooling System

In GRSAC, the 3-D, hexagonal geometry core model uses one node each for 163 fuel and 42 reflector element radial regions in each of 14 axial regions. The annular core representation (205 x 14 = 2870 nodes) thus allows for detailed investigations of azimuthal temperature asymmetries in addition to axial and radial profiles. Variable core thermal properties are computed functions of temperature and are dependent on orientation and radiation damage. An annealing model for graphite accounts for the increase in thermal conductivity that may occur during heatup accidents.

The primary coolant flow models cover the full ranges expected in both normal operation and accidents, including a full range of pressurized and depressurization accidents, for forced and natural circulation, for upflow and downflow, and for turbulent, laminar, and transition flow regimes. The primary loop pressure calculation considers variable inventory (due to depressurization actions) and loop temperature changes and uses a simplified model of balance-of-plant gas temperatures.

B. Anticipated transient without Scram (ATWS) model

In an ATWS event, the expected scram would not occur at the start of an LOFC accident but instead could occur at an arbitrary later time or not at all. Slow rod withdrawal accidents can also be simulated if they are in conjunction with an LOFC accident. The model for fuel (as distinct from moderator) temperature is a quasi-steady state approximation valid only for slow transients characteristic of LOFC accidents. The point kinetics approximation for the neutronics is a prompt-jump, single-precursor-group model that compares favorably, for transients of the appropriate rate and magnitude, with calculations using a "full" model with prompt neutron generation time and six delayed neutron precursor groups included. Temperature-reactivity feedback from the 3-D modeling of fuel, moderator, and reflectors utilizes nuclear importance weighting. Models for xenon and samarium poisoning are included.

C. Graphite oxidation models

At the start of an air ingress oxidation transient, both inlet and outlet plena are assumed to be 100% air (i.e., early diffusion between air and the helium or CO₂ coolant is neglected). Thereafter, oxygen concentrations in the plena are calculated assuming well-stirred tank models. Subsequent inlet gas flow is assumed to be air, which mixes with any oxygen-depleted reverse flows there may be from the core.

Oxygen concentrations are calculated for each node at each time step, accounting for depletion occurring upstream in each flow channel, as well as for oxygen depletion within the time step for each node. All heat from oxidation goes directly into the graphite node. It is assumed that only CO₂ is produced from the oxidation reaction; any CO that is produced would be burned anyway (though perhaps at a different location).

Two alternative oxidation regimes are assumed to exist, and are referred to as Zone I and Zone III oxidation. The Zone I graphite oxidation rate is governed primarily by the intrinsic chemical reactivity of the graphite according to the Arrhenius relationship, $\exp(-E/RT)$. The reaction occurs uniformly throughout an Active Oxidation Zone (AOZ) near the exposed surface. Zone III rates are governed by mass transfer to the exposed surface, where the oxidation occurs. The calculated mass transfer rate is dependent on the degree of turbulence (laminar, transition, and turbulent regimes) and on the diffusion coefficient, which is assumed proportional to the absolute temperature to the 1.8 power. The lesser of the two rates (Zone I or III) is controlling. Oxygen and CO₂ concentration changes in the direction of flow are assumed not to affect air transport properties used for flow and heat/mass transfer correlations.

Experimental data have shown variations of up to a factor of 6 in oxidation rates due to differences in graphite "purity" (the higher the purity, the lower the oxidation rate), and even larger variations due to irradiation and effects of contaminants.

Clad and fuel oxidation modeling, for metal fuel reactor designs, was done in a similar manner to the graphite, but without the AOZ feature.

Iv. Code Verification and Validation Activities

Benchmark cases for steady state conditions, transients, and accidents have been run for comparisons with plant data and with similar codes and simulations developed by others and have shown generally good agreement. Earlier validation exercises using ORECA, a forerunner of MORECA, showed good results in comparisons with transient data from the Fort St. Vrain HTGR [3]. Additional validation efforts are currently under way via international cooperative efforts under the guidance of International Atomic Energy Agency Coordinated Research Programs in the areas of passive decay heat removal, neutronics, and fuel performance.

A.2.3.5. Conclusions

The new ORNL GRSAC code can readily be adapted to simulate a wide variety of GCR designs, and then be used to study a wide range of accidents up through very unlikely, severe accident scenarios. The new enhancements include user-definition capabilities for specific plant designs, "smart front-end" checking of input data, on-line help and documentation, on- and off-line plotting, and an automated sensitivity study option. Continuing work on verification and validation has included both use of experimental data and code-to-code benchmarking.

REFERENCES TO SECTION A.2.3.

- [1] S. J. Ball, MORECA: A Computer Code for Simulating Modular High-Temperature Gas-Cooled Reactor Core Heatup Accidents, NUREG/CR-5712 (ORNL/TM-11823), Oak Ridge National Laboratory, October 1991.
- [2] S. J. Ball and D. J. Nypaver, MORECA-2: Interactive Simulator for Modular High-Temperature Gas-Cooled Reactor Core Transients and Heatup Accidents with ATWS Options, NUREG/CR-5945 (ORNL/TM-12233), Oak Ridge National Laboratory, October 1992.
- [3] S. J. Ball, "Dynamic Model Verification Studies for the Thermal Response of the FSV HTGR Core," Proceedings of the 4th Power Plant Dynamics, Control, and Testing Symposium, The University of Tennessee, Knoxville, 1980.

A.2.4. CFX-F3D Software

A.2.4.1. Description

CFX-F3D [1] flow modelling software performs CFD (Computational Fluid Dynamics) calculations. This software has been developed by AEA technology and solves partial differential conservation equations together with their boundary conditions. For this purpose, the software uses the finite volume method for the discretisation of the Navier-Stokes equations for mass, momentum and energy. A computational grid subdivides the physical domain of the problem geometry into a large number of cells. The governing equations of mass, momentum, and energy conservation are solved for the cell centres. The CFX-F3D software consists of a number of modules. These modules can perform the following tasks:

- the geometry and grid generator may be used to define the finite difference grid;
- the interactive front-end module constructs the data file via a series of menus. The output of this module is a single data file using the command language which represents the problem definition. The command language is a set of English-like commands, subcommands, and associated keywords;
- the front-end module takes the input specification of the problem and converts it into a form designed for efficient execution;
- the solution module solves the discretised representation of the problem;
- the graphics module produces the graphic output.

Release 4.1 of CFX-F3D software has the following features of interest for the present problem:

- multi-block grid capability. This capability involves the use of a set of blocks, which are 'glued' together. For each block there is a structured grid. Boundary conditions, solid regions, and porous regions within the domain are described using the concept of a 'patch';
- heat transfer capabilities. Flows with heat transfer are calculated by adding the equation describing the conservation of energy. However, boundary conditions are defined in terms of temperature or heat flux;
- compressible flow options. The program can solve the equation for the stagnant enthalpy and is therefore valid at all Mach numbers. For flows with Mach number less than about 0.3, there is an option that allows the user to designate the flow to be 'weakly compressible'. This invokes two approximations: the energy equation ignores the kinetic terms, and the speed of sound is assumed to be infinite. These approximations have been found to enhance convergence;
- turbulence models. In addition to the k- ϵ turbulence model which is suitable for high Reynolds number flows, there is a low Reynolds number model. Higher order turbulence models are also available in the software;
- transient flows. Flows varying with time can be modelled.

The radiative heat transfer is modelled in a separate package, called CFX-RADIATION. This package models radiative heat transfer in complex three-dimensional geometries for grey and non-grey systems. Both Monte Carlo and discrete transfer methods are incorporated. CFX-RADIATION can be used as a stand alone package or interfaced with a flow and combustion modelling program such as CFX-F3D.

The following programs have been used for the calculations:

- grid generator: CFX-MESHBUILD;
- solution module: CFX-F3D version 4.1;
- radiation package: CFX-RADIATION;
- graphics module: CFX-VIEW;
- line graph module: CFX-LINEGRAPH;

These programs have been run on a Silicon Graphics Power Challenge workstation.

REFERENCE TO SECTION A.2.4.

- [1] CFX-F3D user guide. Computational Fluid Dynamics Services, Oxfordshire, October 1995.